

## PAPER DETAILS

TITLE: Can Typical Cervical Vertebrae Be Distinguished From One Another By Using Machine Learning Algorithms? Radioanatomic New Markers

AUTHORS: Deniz SENOL,Yusuf SEÇGIN,Seyma TOY,Serkan ÖNER,Zülal ÖNER

PAGES: 210-218

ORIGINAL PDF URL: <https://dergipark.org.tr/tr/download/article-file/2659030>

# RESEARCH ARTICLE

 Deniz Senol<sup>1</sup>  
 Yusuf Secgin<sup>2</sup>  
 Seyma Toy<sup>2</sup>  
 Serkan Oner<sup>3</sup>  
 Zulal Oner<sup>4</sup>

<sup>1</sup> Faculty of Medicine,  
Department of Anatomy, Düzce  
University, Düzce, Türkiye

<sup>2</sup> Faculty of Medicine,  
Department of Anatomy,  
Karabük University, Karabük,  
Türkiye,

<sup>3</sup> Faculty of Medicine,  
Department of Radiology, İzmir  
Bakırçay University, İzmir,  
Türkiye

<sup>4</sup> Faculty of Medicine,  
Department of Anatomy, İzmir  
Bakırçay University, İzmir,  
Türkiye

## Corresponding Author:

Deniz Senol

mail: denianatomi@gmail.com

Received: 19.09.2022

Acceptance: 26.04.2023

DOI: 10.18521/ktd.1177279

Konuralp Medical Journal

e-ISSN1309-3878

konuralptipdergi@duzce.edu.tr

konuralptipdergisi@gmail.com

www.konuralptipdergi.duzce.edu.tr

## Can Typical Cervical Vertebrae Be Distinguished from One Another by Using Machine Learning Algorithms? Radioanatomic New Markers

### ABSTRACT

**Objective:** The aim of this study is to distinguish the typical cervical vertebrae that cannot be separated from one another with the naked eye by using machine algorithms (ML) with measurements made on computerized tomography (CT) images and to show the differences of these vertebrae.

**Methods:** This study was conducted by examining the 536 typical cervical vertebrae CT images of 134 (between the ages of 20 and 55) individuals. Measurements of cervical vertebrae were made on coronal, axial and sagittal section. 6 different combinations (Group 1: C3 – C4, Group 2: C3 – C5, Group 3: C3 – C6, Group 4: C4 – C5, Group 5: C4 – C6, Group 6: C5 – C6) were formed with parameters of each vertebrae and they were analyzed in ML algorithms. Accuracy (Acc), Matthews correlation coefficient (Mcc), Specificity (Spe), Sensitivity (Sen) values were obtained as a result of the analysis.

**Results:** As a result of this study, the highest success was obtained with Linear Discriminant Analysis (LDA) and Logistic Regression (LR) algorithms. The highest Acc rate was found as 0.94 with LDA and LR algorithm in Groups 3 and Group 4, the highest Spe value was found as 0.95 with LDA and LR algorithm in Group 5, the highest Mcc value was found as 0.90 with LDA and LR algorithm in Group 5 and the highest Sen value was found as 0.94 with LDA and LR algorithm in Groups 3 and 5.

**Conclusions:** As a conclusion, it was found that typical cervical vertebrae can be distinguished from each other with high accuracy by using ML algorithms.

**Keywords:** Typical Cervical Vertebrae, Machine Learning Algorithms, Computerized Tomography.

## Tipik Servikal Omurlar Makine Öğrenimi Algoritmaları Kullanılarak Birbirinden Ayırt Edilebilir mi? Radyoanatomik Yeni Belirteçler

### ÖZET

**Amaç:** Bu çalışmanın amacı, bilgisayarlı tomografi (BT) görüntülerinde yapılan ölçümlerle makine algoritmaları (ML) kullanılarak çıplak gözle birbirinden ayıramayan tipik servikal omurları ayırt etmek ve bu omurların farklılıklarını göstermektir.

**Gereç ve Yöntem:** Bu çalışma 134 (20-55 yaş arası) bireyin 536 tipik servikal vertebra BT görüntüleri incelenerek yapıldı. Servikal vertebraların koronal, aksiyal ve sagittal kesitlerinde ölçümleri yapıldı. Parametrelerle 6 farklı kombinasyon (Grup 1: C3 – C4, Grup 2: C3 – C5, Grup 3: C3 – C6, Grup 4: C4 – C5, Grup 5: C4 – C6, Grup 6: C5 – C6) oluşturulup her bir omur ML algoritmalarında analiz edildi. Analiz sonucunda Doğruluk (Acc), Matthews korelasyon katsayısı (Mcc), Özgüllük (Spe), Duyarlılık (Sen) değerleri elde edildi.

**Bulgular:** Bu çalışma sonucunda en yüksek başarı Linear Discriminant Analysis (LDA) ve Logistic Regresyon (LR) algoritmaları ile elde edildi. Grup 3 ve Grup 4'te en yüksek Acc oranı LDA ve LR algoritması ile 0.94, en yüksek Spe değeri Grup 5'te LDA ve LR algoritması ile 0.95, en yüksek Mcc değeri LDA ve LR algoritması ile 0.90 olarak bulundu. Grup 5'te en yüksek Sen değeri, Grup 3 ve 5'te LDA ve LR algoritması ile 0.94 olarak bulundu.

**Sonuç:** Sonuç olarak, tipik servikal vertebraların ML algoritmaları kullanılarak birbirinden yüksek doğruluk oranı ile ayırt edilebildiği bulundu.

**Anahtar Kelimeler:** Tipik Servikal Omurga, Makine Öğrenimi Algoritmaları, Bilgisayarlı Tomografi.

## INTRODUCTION

Vertebral column is an important anatomical structure that is connected to intervertebral disc, formed by the combination of 33 vertebrae, extending from cranium to coccyx (1). The part of this structure in the neck region is called cervical vertebrae and there are 7 of these. Cervical vertebrae 1, 2 and 7 are called atypical, while the others are called typical. Although the basic features of typical vertebrae are the same, their sizes can vary and therefore they can show unique morphometric differences (2).

Cervical vertebrae surgery goes back to 1500s B.C. Although surgical intervention technologies in this area have made significant process up till now, many complications can still occur (3-5). The main reason for these complications is that the complex anatomy of cervical vertebrae limits surgical intervention. The close neighbourhood of cervical vertebrae to vital structures such as vertebral artery, spinal cord and spinal nerves create serious difficulties for surgeons performing interventional procedures in this region (6). It has been reported that transpedicular screw fixation is a surgical procedure that might create confusion for the cervical region and this practice becomes much more complex with the pedicular length and width that changes from individual to individual (7-9). Understanding the relationship between pedicle size and shape and vital adjacent structures increases the reliability of transpedicular screw fixation (10-15).

It has been reported in literature that the positions of vertebrae can be determined with intraoperative computed tomography (iCT) based systems by using intraoperative neuro-navigation methods and with this method, incorrect location of the screw to be used in the cervical area can be prevented (16). Although this information increases the safety of patient based operation, it may not be applied in all centres. This situation shows the importance of clarifying cervical vertebrae morphometry radioanatomically and distinguishing between typical cervical vertebrae.

Machine learning (ML) algorithms which have emerged with the close relationship of mathematics and computer science and it can be seen that they have begun to be used in the field of medicine and important results have been obtained today (17-21). Decision Tree (DT) is an algorithm that tries to find the estimators with the highest distinguishing feature by subdividing the relationships among multiple independent variables (22). Random Forest (RF) is an algorithm that shows higher accuracy in estimating nonlinear and complex data (23). Logistic regression (LR) is an algorithm that can highly predict and classify categorical data (24). Linear discriminant analysis (LDA) is an algorithm that can reveal the

contribution of each parameter in the data set to the overall result (25). Quadratic discriminant analysis (QDA) is a parametric classifier algorithm with higher efficiency than LDA. Extra Tree Classifier (ETC) is a tree algorithm that randomly splits nodes (26).

The aim of this study is to show on CT images the morphometric differences of typical cervical vertebrae which are very similar and difficult to distinguish with the naked eye and to try to distinguish between these vertebrae by using ML algorithms.

## MATERIAL AND METHODS

**Population and Image Samples:** The present study was initiated with the 2021/484 numbered decision of Karabük University Non-Interventional Ethics Committee. 536 cervical CT images of a total of 134 individuals between the ages of 20 and 55 were included in the study.

**Multidetector CT (MDCT) Protocol:** The images were obtained by using 16 row multidetector computed tomography (Aquilion 16; Toshiba Medical Systems, Otawara, Japan) at Karabük University Training and Research Hospital Department of Radiology. Screening protocol values were found as pitch: 1.0 mm, tube voltage: 120 kV, gantry rotation: 0.75 s and image section thickness value: 1 mm.

**Image Analysis:** The images in Digital Imaging and Communications in Medicine (DICOM) format were transferred to Horos Medical Image Viewer (Version 3.0, USA) program and images were obtained in axial, coronal and sagittal plane by using 3D Curved Multiplanar Reconstruction (MPR). The line passing through the middle of vertebral body and spinous process was determined and all images were brought to orthogonal plane (Figure 1).

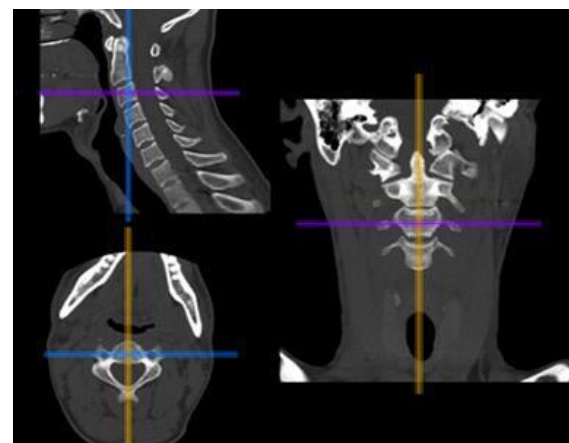


**Figure 1.** Method of bringing C3 vertebrae to orthogonal plane.

Length and angle measurements of certain anatomical points were made through MDCT brought to orthogonal plane (Figure 2).

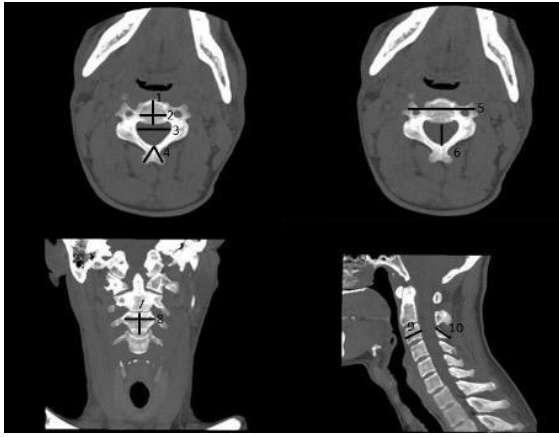


**Figure 2.** Measurements for C3 vertebrae on axial, coronal and sagittal plane (on axial image; 1: anterior posterior length of the vertebral body, 2: transverse length of the vertebral body, 3: transverse length of the vertebral foramen, 4: spinous process angle, 5: the distance between transverse processes, 6: anterior posterior length of the vertebral foramen; on coronal image; 7: vertebral body height, 8: vertebral body width; on sagittal image; 9: vertebral body thickness, 10: spinous process length measurement)

Measurement parameters were anterior posterior length of the vertebral body, transverse length of the vertebral body, transverse length of the vertebral foramen, spinous process angle, the distance between transverse processes and anterior posterior length of the vertebral foramen on axial section; vertebral body height and vertebral body width measurements on coronal section and vertebral body thickness and spinous process length measurement on sagittal section.

**ML Algorithms:** ML algorithms were performed by using an Hp-Folio 1040 model computer with i7 operating system and 8 Gb Ram. Python programming language (version 3.7.1) and scikit-learn library (version 0.20.0) were used for ML modelling (27). DT, RF, LR, LDA, QDA, ETC

algorithms were used. Training set was determined as 80%, while test set was determined as 20%. In addition, groups of two were formed for each cervical vertebrae and analyses were made on these groups (Table 1).

**Table 1.** ML algorithms analysis groups

Analysis groups	
Group 1	C3 – C4
Group 2	C3 – C5
Group 3	C3 – C6
Group 4	C4 – C5
Group 5	C4 – C6
Group 6	C5 – C6

**Performance Criteria:** Accuracy (Acc), Matthews correlation coefficient (Mcc), Specificity (Spe), Sensitivity (Sen), F1 score (F1) values were used in this study.

$$Acc = \frac{TP}{TP+FN+FP+TN}$$

$$Mcc = \frac{TP \times TN - FP \times FN}{\sqrt{(TP+FP) \times (TP+FN) \times (TN+FP) \times (TN+FN)}}$$

$$Sen = \frac{TP}{TP+FN}$$

$$Spe = \frac{TN}{TN+FP}$$

$$F1 = 2 \frac{Spe \times Sen}{Spe+Sen}$$

**Equation 1.** (FP; False positive, FN; False negative, TP; True positive, TN; True negative)

**Statistical Analysis:** Mean and standard deviation values were used in the descriptive statistics of each cervical vertebrae. Minitab 17 program was used for descriptive statistics.

## RESULTS

Parameters obtained from 134 analyzed images and descriptive statistical analyses obtained from C3, C4, C5 and C6 are shown in (Table 2, 3, 4, 5).

**Table 2.** C3 vertebrae descriptive statistics

Parameters (C3)	Sex	Mean	SD
Anterior posterior length of the vertebral body (cm)	Male	2.173	0.194
	Female	2.036	0.178
Transverse length of the vertebral body (cm)	Male	1.318	0.124
	Female	1.181	0.172
Transverse length of the vertebral foramen (cm)	Male	2.565	0.202
	Female	2.417	0.161
Spinous process angle (°)	Male	35.590	10.970
	Female	38.830	11.200
The distance between transverse processes (cm)	Male	4.767	0.301
	Female	4.320	0.181
Anterior posterior length of the vertebral foramen (cm)	Male	1.456	0.188
	Female	1.411	0.138
Vertebral body height (cm)	Male	1.640	0.298
	Female	1.445	0.191
Vertebral body width (cm)	Male	2.536	0.233
	Female	2.399	0.184
Vertebral body thickness (cm)	Male	1.617	0.130
	Female	1.384	0.239
Spinous process length (cm)	Male	1.964	0.368
	Female	1.606	0.299

**Table 3.** C4 vertebrae descriptive statistics

Parameters (C4)	Sex	Mean	SD
Anterior posterior length of the vertebral body (cm)	Male	2.165	0.210
	Female	2.013	0.168
Transverse length of the vertebral body (cm)	Male	1.376	0.146
	Female	1.202	0.144
Transverse length of the vertebral foramen (cm)	Male	2.810	0.305
	Female	2.619	0.202
Spinous process angle (°)	Male	40.590	13.560
	Female	42.870	11.310
The distance between transverse processes (cm)	Male	4.748	0.499
	Female	4.373	0.186
Anterior posterior length of the vertebral foramen (cm)	Male	1.440	0.242
	Female	1.338	0.159
Vertebral body height (cm)	Male	1.557	0.304
	Female	1.359	0.136
Vertebral body width (cm)	Male	2.656	0.254
	Female	2.440	0.157
Vertebral body thickness (cm)	Male	1.621	0.139
	Female	1.419	0.120
Spinous process length (cm)	Male	2.030	0.734
	Female	1.721	0.236

**Table 4.** C5 vertebrae descriptive statistics

Parameters (C5)	Sex	Mean	SD
Anterior posterior length of the vertebral body (cm)	Male	2.308	0.243
	Female	2.066	0.186
Transverse length of the vertebral body (cm)	Male	1.367	0.146
	Female	1.214	0.138
Transverse length of the vertebral foramen (cm)	Male	2.876	0.305
	Female	2.704	0.174
Spinous process angle (°)	Male	36.780	10.810
	Female	35.230	9.420
The distance between transverse processes (cm)	Male	4.645	0.272
	Female	4.309	0.175
Anterior posterior length of the vertebral foramen (cm)	Male	1.483	0.264
	Female	1.356	0.179
Vertebral body height (cm)	Male	1.451	0.241
	Female	1.281	0.136
Vertebral body width (cm)	Male	2.753	0.210
	Female	2.548	0.175
Vertebral body thickness (cm)	Male	1.587	0.152
	Female	1.406	0.121
Spinous process length (cm)	Male	2.227	0.357
	Female	1.857	0.249

**Table 5.** C6 vertebrae descriptive statistics

Parameters (C6)	Sex	Mean	SD
Anterior posterior length of the vertebral body (cm)	Male	2.544	0.290
	Female	2.311	0.237
Transverse length of the vertebral body (cm)	Male	1.475	0.191
	Female	1.265	0.129
Transverse length of the vertebral foramen (cm)	Male	2.822	0.219
	Female	2.697	0.180
Spinous process angle (°)	Male	20.935	5.232
	Female	22.891	4.515
The distance between transverse processes (cm)	Male	4.783	0.297
	Female	4.439	0.194
Anterior posterior length of the vertebral foramen (cm)	Male	1.456	0.216
	Female	1.402	0.216
Vertebral body height (cm)	Male	1.454	0.267
	Female	1.264	0.135
Vertebral body width (cm)	Male	2.932	0.261
	Female	2.699	0.204
Vertebral body thickness (cm)	Male	1.666	0.183
	Female	1.456	0.120
Spinous process length (cm)	Male	2.723	0.525
	Female	2.394	0.363

As a result of ML algorithm analysis, the highest Acc value was found in groups 3 and 5 as 0.94 with LDA and LR algorithms (Table 6).

As a result of ML algorithm analysis, the highest Mcc was found in group 3 as 0.90 with LDA and LR algorithms (Table 7).

**Table 6.** ML algorithms Acc table

MLA	Group 1	Group 2	Group 3	Group 4	Group 5	Group 6
DT	68.52	74.07	90.74	68.52	90.74	85.19
RF	<b>77.78</b>	85.19	92.53	<b>81.48</b>	90.74	81.48
ETC	55.56	75.93	87.04	70.37	85.19	74.07
LDA	70.37	88.89	<b>94.44</b>	77.78	<b>94.44</b>	83.33
QDA	48.15	55.56	77.78	75.93	92.59	<b>90.74</b>
LR	74.07	<b>90.47</b>	<b>94.44</b>	79.63	<b>94.44</b>	85.16

**Table 7.** ML algorithms Mcc table

MLA	Group 1	Group 2	Group 3	Group 4	Group 5	Group 6
DT	37.4	48.1	81.5	37.2	81.5	70.6
RF	<b>55.8</b>	70.6	85.2	<b>63.0</b>	81.5	63.2
ETC	12.5	52.3	74.1	40.9	70.4	48.4
LDA	41.4	77.7	<b>88.9</b>	55.5	<b>89.5</b>	66.7
QDA	00.7	27.3	62.5	52.3	85.4	<b>82.0</b>
LR	48.9	<b>81.5</b>	<b>88.9</b>	59.2	<b>89.5</b>	70.3

As a result of ML algorithm analysis, the highest Spe value was found in groups 3 and 5 as 0.95 with LDA and LR algorithms (Table 8).

As a result of ML algorithm analysis, the highest Sen value was found in groups 3 and 5 as 0.94 with LDA and LR algorithms (Table 9).

**Table 8.** ML algorithms Spe table

MLA	Group 1	Group 2	Group 3	Group 4	Group 5	Group 6
DT	68.9	74.1	90.8	69.0	90.8	85.4
RF	<b>78.0</b>	85.4	92.6	<b>81.6</b>	90.8	81.7
ETC	56.6	76.3	87.1	70.6	85.3	74.3
LDA	71.0	88.9	<b>94.5</b>	77.8	<b>95.0</b>	83.4
QDA	49.1	76.9	84.8	76.3	92.8	<b>91.3</b>
LR	74.8	<b>90.8</b>	<b>94.5</b>	79.6	<b>95.0</b>	85.2

**Table 9.** ML algorithms Sen table

MLA	Group 1	Group 2	Group 3	Group 4	Group 5	Group 6
DT	68.5	74.1	90.7	68.5	90.7	85.2
RF	<b>77.8</b>	85.2	92.6	<b>81.5</b>	90.7	81.5
ETC	55.6	75.9	87.0	70.4	85.2	74.1
LDA	70.4	88.9	<b>94.4</b>	77.8	<b>94.4</b>	83.3
QDA	48.1	55.6	77.8	75.9	92.6	<b>90.7</b>
LR	74.1	<b>90.7</b>	<b>94.4</b>	79.6	<b>94.4</b>	85.2

Confusion Matrix table was included for LDA and LR algorithms of group 3 (C3-C6) and group 5 (C4-C6) which had the highest accuracy rate. For group 3, 26 of C3 vertebrae were predicted correctly, while 2 were predicted incorrectly and 25

of C6 vertebrae were predicted correctly, while 2 were predicted incorrectly (Figure 3).

For group 5, 25 of C4 vertebrae were predicted correctly, while 3 were predicted incorrectly and all of C6 vertebrae were predicted correctly (Figure 4).

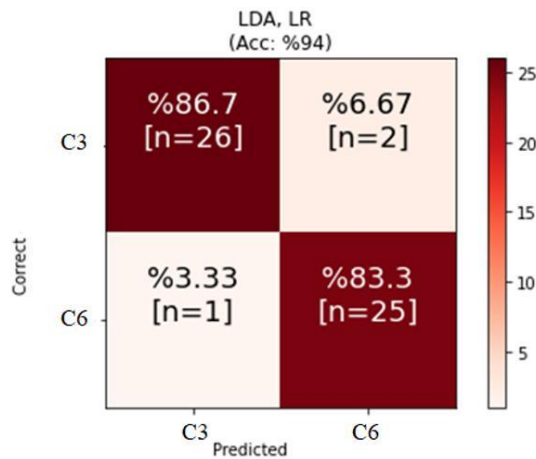


**Figure 3.** Group 3 Confusion Matrix table

In addition, in our study, the SHAP analyzer of the RF algorithm was applied to group 3 to reveal the contribution of the parameters to the algorithm. This group was preferred because group

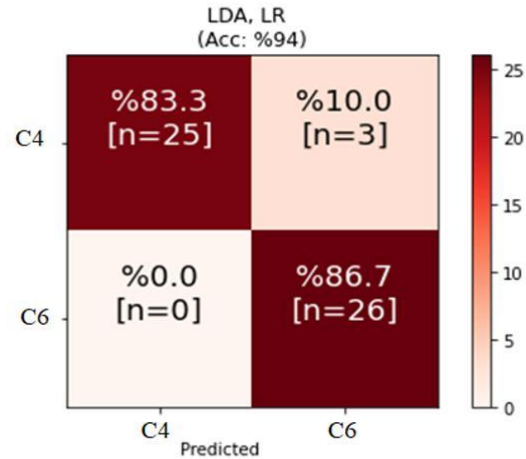


**Figure 4.** Group 5 Confusion Matrix table

3 had the highest Acc rate with the RF algorithm. As a result of the SHAP analyzer, it was found that the spinous process angle parameter provided the highest contribution (Figure 5).

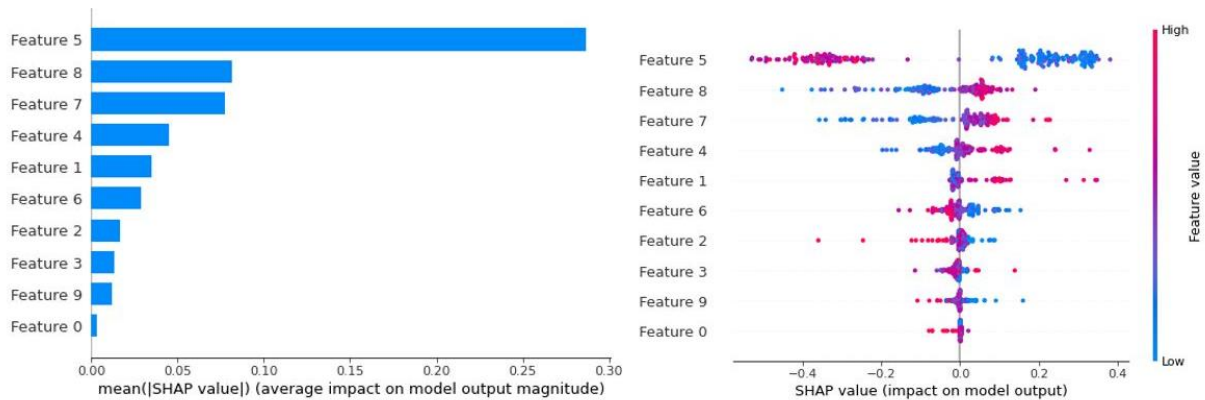


**Figure 5:** SHAP explanatory of RF algorithm (Feature 5: Spinous process angle, Feature 8: Spinous process length measurement, Feature 7: Vertebral body width; on sagittal image, Feature 4: Transverse length of the vertebral foramen, Feature 1: Transverse length of the vertebral body, Feature 6: Cervical body height; on sagittal image, Feature 2: The distance between transverse processes, Feature 3: Anterior posterior length of the vertebral foramen, Feature 9: Vertebral body thickness, Feature 0: Anterior posterior length of the vertebral body)

## DISCUSSION

The aim of this study was to analyze typical cervical vertebrae by using morphometric measurements taken from CT images and to distinguish typically known cervical vertebrae from one another. As a result of the study, the highest Acc rate was found as 0.94 with LDA and LR algorithm in group 3 (C3-C6) and group 5 (C4-C6); the highest Spe value was found as 0.95 with LDA and LR algorithm in group 5, the highest Mcc value was found as 0.90 with LDA and LR algorithm in group 5 (C4-C6) and the highest Sen value was found as 0.94 with LDA and LR algorithm in group 3 (C3-C6) and 5 (C4-C6).

Lack of micro level anatomical and radio-anatomical studies defining cervical vertebrae anatomy may be the main reason why many clinicians are concerned about the application of the transpedicular screw fixation technique in subaxial cervical shoulder area (8, 28, 29). Due to its unique

structure and important neural relationships, cervical vertebrae orientation and accurate correct anatomical knowledge are important to safely perform surgeries of this area (30, 31). For this reason, it can be seen that a large number of studies have been conducted to increase the level of anatomical knowledge of the cervical area in literature.

It is known that cervical vertebrae morphology is examined in detail with analyses made from cadaver and by using dry bone and computed tomography images (10-15).

However, the relationship between these osteometric measurements could not be fully demonstrated and it can be seen that there is no consensus in the results. CT is a radiological tool that can show all tissues and especially bone tissue with sharp boundaries and thus due to being less affected by orientation in length and angle

measurements, it is superior to conventional osteometric measurements (17, 18, 26).

In typical cervical vertebrae measurements they conducted with dry bones, Pramela et al. (32) found mean length of the vertebral body as  $10.92 \pm 1.35$  mm, mean anterior posterior length of the vertebral foramen as  $12.33 \pm 1.68$  mm, mean transverse length of the vertebral body as  $23.22 \pm 2.16$  mm, and mean anterior posterior length of the vertebral body as  $14.79 \pm 1.96$  mm. In the present study, we found vertebral body height as  $1.640 \pm 0.298$  cm in male and  $1.445 \pm 0.191$  cm in female on coronal image of C3 vertebrae; as  $1.557 \pm 0.304$  cm in male and  $1.359 \pm 0.136$  cm in female on C4 vertebrae; as  $1.451 \pm 0.241$  cm in male and  $1.281 \pm 0.136$  cm in female on C5 vertebrae and as  $1.454 \pm 0.267$  cm in male and  $1.264 \pm 0.135$  cm in female on C6 vertebrae. Studies have evaluated morphometric characteristics of typical cervical vertebrae and these results support our results. However, the main purpose of our study is to focus on micro-anatomical differences between typical cervical vertebrae besides their morphometric characteristics and to be a guide to physicians who carry out surgical interventions in the field.

In their study conducted with CT images of dry bones, Gupta et al. (33) found transverse length of the vertebral foramen as  $20.89 \pm 1.65$  mm on C3, as  $21.94 \pm 1.48$  mm on C4, as  $21.96 \pm 1.52$  mm on C5 and as  $22.31 \pm 1.78$  mm on C6. Pramela et al. (32) found transverse length of the vertebral foramen as  $21.98 \pm 1.82$  mm, while Kayalıoğlu et al. (11) found as 18.5 mm and 25.7 mm. In the radiological study they conducted with adults, Çevirgen et al. (34) found transverse length of the vertebral foramen as  $25.4 \pm 1.6$  mm in male and  $26 \pm 2.4$  mm in female for C3, as  $26.1 \pm 2.1$  mm in male and  $26.4 \pm 2$  mm in female for C4, as  $26 \pm 4.5$  mm in male and  $26.5 \pm 1.2$  mm in female for C5 and as  $27.2 \pm 1.9$  mm in male and  $27.2 \pm 1.9$  mm in female for C6. In the present study, on axial image we found transverse length of the vertebral foramen as  $2.565 \pm 0.202$  cm in male and  $2.417 \pm 0.101$  cm in female for C3 vertebrae, as  $2.810 \pm 0.305$  cm in male and  $2.619 \pm 0.202$  cm in female for C4 vertebrae, as  $2.876 \pm 0.305$  cm in male and  $2.704 \pm 0.174$  cm in female for C5 vertebrae and as  $2.822 \pm 0.219$  cm in male and  $2.697 \pm 0.180$  cm in female for C6 vertebrae. Results obtained with CT images of dry bones support the results of our study.

In their study conducted on cadaver, Uğur et al. (35) found transverse length of the vertebral foramen as 21.86 mm for C3, as 21.1 mm for C4, as 21.2 mm for C5 and as 22.3 mm for C6. The results for transverse length of the vertebral foramen were similar in the present study.

## REFERENCES

1. Saluja S, Patil S, Vasudeva N. Morphometric Analysis of Sub-axial Cervical Vertebrae and Its Surgical Implications. *J Clin Diagn Res.* 2015;9(11):AC01-4.

On CT images Evangelopoulos et al. (36) found anterior posterior length of the vertebral foramen as  $13.31 \pm 1.71$  mm in male and as  $12.94 \pm 1.32$  mm in female for C3, as  $13.05 \pm 1.01$  mm in male and as  $12.49 \pm 1.49$  mm in female for C4, as  $13.43 \pm 1.22$  mm in male and as  $12.66 \pm 1.68$  mm in female for C5 and as  $13.28 \pm 1.85$  mm in male and as  $12.52 \pm 1.76$  mm in female for C6. In the radiological study they conducted on adults, Çevirgen et al. (34) found anterior posterior length of the vertebral foramen as  $15.9 \pm 1.7$  mm in male and  $16 \pm 1.5$  mm in female for C3, as  $15.5 \pm 1.8$  mm in male and  $16 \pm 1$  mm in female for C4, as  $16 \pm 2.1$  mm in male and  $16.3 \pm 1.3$  mm in female for C5 and as  $16.5 \pm 2.3$  mm in male and  $16.7 \pm 1.5$  mm in female for C6. In our study, on axial images, anterior posterior length of the vertebral foramen was found as  $1.456 \pm 0.188$  cm in male and  $1.411 \pm 0.138$  cm in female for C3 vertebrae, as  $1.440 \pm 0.242$  cm in male and  $1.338 \pm 0.159$  cm in female for C4 vertebrae, as  $1.483 \pm 0.264$  cm in male and  $1.356 \pm 0.179$  cm in female for C5 vertebrae and as  $1.456 \pm 0.216$  cm in male and  $1.402 \pm 0.216$  cm in female for C6 vertebrae.

In a radiological study they conducted with CT in Poland, Ludwisiak et al. (37) measured spinous process angle as  $27.8^\circ$  for C3, as  $30.3^\circ$  for C4, as  $29^\circ$  for C5 and as  $26^\circ$  for C6. They also evaluated spinous process angle between the two ends and found as  $35.590^\circ$  in male and  $38.830^\circ$  in female for C3 vertebrae, as  $40.590^\circ$  in male and  $42.870^\circ$  in female for C4 vertebrae, as  $36.780^\circ$  in male and  $35.230^\circ$  in female for C5 vertebrae and as  $20.935^\circ$  in male and  $22.891^\circ$  in female for C6 vertebrae on axial image. We believe that the differences in angle measurements are due to differences in populations.

In our study, CT imaging technology was preferred as it provides three dimensional imaging, reconstruction and a large database in addition to classical osteometric methods. In addition, the biggest difference that distinguishes our study from the others is the ML algorithms used and the result that morphometric features of cervical vertebrae which are considered as typical can be distinguished from each other.

## CONCLUSION

To the best of our knowledge, this is the first study that can distinguish typical cervical vertebrae from one another by using ML algorithms and CT imaging technology together. For this reason, we believe that our study will provide important contributions to literature, anatomists and surgeons.



2. Desdicioglu K, Öztürk K, Çizmeçi G, Malas M. Morphometric investigation of anatomic structures of vertebrae and clinical evaluation: an anatomical study. *SDU Sağlık Bilimleri Dergisi*. 2017;8(1):16-20.
3. Dweik A, Van den Brande E, Kossman T, Maas AI. History of cervical spine surgery: from nihilism to advanced reconstructive surgery. *Spinal Cord*. 2013;51(11):809-14.
4. Wang T, Wang H, Liu S, Ding WY. Incidence of C5 nerve root palsy after cervical surgery: A meta-analysis for last decade. *Medicine (Baltimore)*. 2017;96(45):e8560.
5. Neo M, Fujibayashi S, Miyata M, Takemoto M, Nakamura T. Vertebral artery injury during cervical spine surgery: a survey of more than 5600 operations. *Spine (Phila Pa 1976)*. 2008;33(7):779-85.
6. Nottmeier EW, Pirris SM, Edwards S, Kimes S, Bowman C, Nelson KL. Operating room radiation exposure in cone beam computed tomography-based, image-guided spinal surgery: clinical article. *J Neurosurg Spine*. 2013;19(2):226-31.
7. Kothe R, Ruther W, Schneider E, Linke B. Biomechanical analysis of transpedicular screw fixation in the subaxial cervical spine. *Spine (Phila Pa 1976)*. 2004;29(17):1869-75.
8. Ebraheim NA, Xu R, Knight T, Yeasting RA. Morphometric evaluation of lower cervical pedicle and its projection. *Spine (Phila Pa 1976)*. 1997;22(1):1-6.
9. Bailey AS, Stanescu S, Yeasting RA, Ebraheim NA, Jackson WT. Anatomic relationships of the cervicothoracic junction. *Spine (Phila Pa 1976)*. 1995;20(13):1431-9.
10. Bozbuga M, Ozturk A, Ari Z, Sahinoglu K, Bayraktar B, Cecen A. Morphometric evaluation of subaxial cervical vertebrae for surgical application of transpedicular screw fixation. *Spine (Phila Pa 1976)*. 2004;29(17):1876-80.
11. Kayalioglu G, Erturk M, Varol T, Cezayirli E. Morphometry of the cervical vertebral pedicles as a guide for transpedicular screw fixation. *Neurol Med Chir (Tokyo)*. 2007;47(3):102-7; discussion 7-8.
12. Sakamoto T, Neo M, Nakamura T. Transpedicular screw placement evaluated by axial computed tomography of the cervical pedicle. *Spine (Phila Pa 1976)*. 2004;29(22):2510-4; discussion 5.
13. Shin EK, Panjabi MM, Chen NC, Wang JL. The anatomic variability of human cervical pedicles: considerations for transpedicular screw fixation in the middle and lower cervical spine. *Eur Spine J*. 2000;9(1):61-6.
14. Vara CS, Thompson GH. A cadaveric examination of pediatric cervical pedicle morphology. *Spine (Phila Pa 1976)*. 2006;31(10):1107-12.
15. Yusof MI, Ming LK, Abdullah MS, Yusof AH. Computerized tomographic measurement of the cervical pedicles diameter in a Malaysian population and the feasibility for transpedicular fixation. *Spine (Phila Pa 1976)*. 2006;31(8):E221-4.
16. Kirnaz S, Gebhard H, Wong T, Nangunoori R, Schmidt FA, Sato K, et al. Intraoperative image guidance for cervical spine surgery. *Ann Transl Med*. 2021;9(1):93.
17. Secgin Y, Oner Z, Turan MK, Oner S. Gender prediction with parameters obtained from pelvis computed tomography images and decision tree algorithm. *Medicine Science International Medical Journal*. 2021;10(2):356-61.
18. Secgin Y, Oner Z, Turan MK, Oner S. Gender prediction with the parameters obtained from pelvis computed tomography images and machine learning algorithms. *Journal of the Anatomical Society of India*. 2022;71(3):204.
19. Deo RC. Machine Learning in Medicine. *Circulation*. 2015;132(20):1920-30.
20. Erickson BJ, Korfiatis P, Akkus Z, Kline TL. Machine Learning for Medical Imaging. *Radiographics*. 2017;37(2):505-15.
21. Senol D, Bodur F, Seçgin Y, Bakıcı R, Sahin N, Toy S, et al. Sex prediction with morphometric measurements of first and fifth metatarsal and phalanx obtained from X-ray images by using machine learning algorithms. *Folia Morphologica*. 2022.
22. Reges O, Krefman AE, Hardy ST, Yano Y, Muntner P, Lloyd-Jones DM, et al. Decision Tree-Based Classification for Maintaining Normal Blood Pressure Throughout Early Adulthood and Middle Age: Findings From the Coronary Artery Risk Development in Young Adults (CARDIA) Study. *American journal of hypertension*. 2021;34(10):1037-41.
23. Sarica A, Cerasa A, Quattrone A. Random forest algorithm for the classification of neuroimaging data in Alzheimer's disease: a systematic review. *Frontiers in aging neuroscience*. 2017;9:329.
24. DeGregory K, Kuiper P, DeSilvio T, Pleuss J, Miller R, Roginski J, et al. A review of machine learning in obesity. *Obesity reviews*. 2018;19(5):668-85.
25. Perfecto-Avalos Y, Garcia-Gonzalez A, Hernandez-Reynoso A, Sánchez-Ante G, Ortiz-Hidalgo C, Scott S-P, et al. Discriminant analysis and machine learning approach for evaluating and improving the performance of immunohistochemical algorithms for COO classification of DLBCL. *Journal of translational medicine*. 2019;17(1):1-12.
26. Toy S, Secgin Y, Oner Z, Turan MK, Oner S, Senol D. A study on sex estimation by using machine learning algorithms with parameters obtained from computerized tomography images of the cranium. *Scientific Reports*. 2022;12(1):1-11.

27. Pedregosa F, Varoquaux G, Gramfort A, Michel V, Thirion B, Grisel O, et al. Scikit-learn: Machine learning in Python. *the Journal of machine Learning research*. 2011;12:2825-30.
28. Jeanneret B, Gebhard JS, Magerl F. Transpedicular screw fixation of articular mass fracture-separation: results of an anatomical study and operative technique. *J Spinal Disord*. 1994;7(3):222-9.
29. Xu R, Kang A, Ebraheim NA, Yeasting RA. Anatomic relation between the cervical pedicle and the adjacent neural structures. *Spine (Phila Pa 1976)*. 1999;24(5):451-4.
30. Jones EL, Heller JG, Silcox DH, Hutton WC. Cervical pedicle screws versus lateral mass screws. Anatomic feasibility and biomechanical comparison. *Spine (Phila Pa 1976)*. 1997;22(9):977-82.
31. Kotani Y, Cunningham BW, Abumi K, McAfee PC. Biomechanical analysis of cervical stabilization systems. An assessment of transpedicular screw fixation in the cervical spine. *Spine (Phila Pa 1976)*. 1994;19(22):2529-39.
32. Pameela M, Prabhu LV, Murlimanju B, Pai MM, Rai R-I, Kumar CG. Anatomical dimensions of the typical cervical vertebrae and their clinical implications. *Eur j anat*. 2020;9-15.
33. Gupta R, Kapoor K, Sharma A, Kochhar S, Garg R. Morphometry of typical cervical vertebrae on dry bones and CT scan and its implications in transpedicular screw placement surgery. *Surg Radiol Anat*. 2013;35(3):181-9.
34. Cevirgen F, Karaca L, Senol D, Cetin A, Ozbag D. Analysis in terms of gender of morphometric characteristics of typical cervical vertebrae: A radiological study. *Med Sci*. 2018;7:355-9.
35. Ugur HC, Attar A, Uz A, Tekdemir I, Egemen N, Caglar S, et al. Surgical anatomic evaluation of the cervical pedicle and adjacent neural structures. *Neurosurgery*. 2000;47(5):1162-8; discussion 8-9.
36. Evangelopoulos D, Kontovazenis P, Kouris S, Zlatidou X, Benneker L, Vlamis J, et al. Computerized tomographic morphometric analysis of the cervical spine. *Open Orthop J*. 2012;6:250-4.
37. Ludwisiak K, Podgorski M, Biernacka K, Stefanczyk L, Olewnik L, Majos A, et al. Variation in the morphology of spinous processes in the cervical spine - An objective and parametric assessment based on CT study. *PLoS One*. 2019;14(6):e0218885.